Effects of the hydroelectric developments on the oceanographic surface parameters of Hudson Bay

S.J. Prinsenberg

Effects of the Hydroelectric Developments on the Oceanographic Surface Parameters of Hudson Bay

S.J. Prinsenberg
Ocean Science and Surveys
Burlington, Ontario

ABSTRACT *A one-dimensional oceanic mixed-layer model was used to simulate the annual surface layer properties of Hudson Bay. The model reproduces the sparse available data well and shows the equal importance of seasonal ice cover and run-off on the pycnocline pattern. In spring, the large freshwater input from run-off and local ice melt followed by summer heating slows the deepening of the pycnocline depth by wind mixing. As these stabilizing effects decrease and the wind strength increases, the pycnocline depth increases in the fall and continues to increase in the winter when the salt rejection effect during ice growth replaces the cooling effect. In the spring the salt rejection reduces and run-off increases; the large pycnocline depth cannot be maintained and a shallow pycnocline is formed, starting a new seasonal cycle.*

When the run-off cycle includes the effects of hydroelectric developments, the results indicate that a new shallow surface pycnocline is formed earlier in the spring. This causes a decrease in surface layer temperature and salinity, thus stimulating more ice growth. On the other hand, in the summer the surface layer salinity is higher and the temperature lower. This decreases the stability, thus further deepening the pycnocline and increasing the deviations from normal conditions.

RÉSUMÉ *Un modèle océanographique à dimension unique et à couche de mélange, a été utilisé pour simuler les propriétés annuelles de la couche en surface de la Baie d'Hudson. Le modèle reproduit adéquatement les données éparses disponibles et démontre l'importance égale de la couverture de la glace saisonnière à celle du ruissellement sur la configuration de la pycnocline. Au printemps, l'apport d'eau douce du ruissellement et de la fonte de la glace, suivi par le réchauffement estival, ralentissent le développement de l'épaisseur de la pycnocline grâce au mélange par le vent. Au fur et à mesure que ces effets stabilisateurs diminuent, et que l'intensité du vent augmente, la profondeur de la pycnocline augmente à l'automne et continue à augmenter en hiver lorsque l'effet du rejet du sel au cours de la croissance de la glace remplace l'effet du refroidissement. Au printemps le rejet du sel diminue et le ruissellement augmente; la profondeur considérable de la pycnocline ne peut pas être maintenue et une pycnocline peu profonde est formée, recommençant ainsi un nouveau cycle saisonnier.*

Lorsque l'effet de l'expansion des centrales hydroélectriques est inclus dans le cycle du ruissellement, les résultats indiquent qu'une nouvelle couche peu profonde de la pycnocline en surface se forme plus tôt dans le printemps. Ceci résulte en un décroissement dans la température et de la salinité de la couche en surface, stimulant ainsi la croissance de plus de

glace. En été d'autre part, la salinité de la couche en surface est plus élevée et la température est moins élevée. Ceci diminue la stabilité, ce qui épaissit plus encore la pycnocline et intensifie l'écart des conditions normales.

---

1 Introduction

This paper describes the application of a simple wind-mixed layer model to Hudson Bay using present and future run-off conditions. Although Hudson Bay is a large inland sea, the history of intensive oceanographic studies of the area is short. Initial investigations of the distribution of properties (Barber, 1967) and heat fluxes (Danielson, 1969) were done in the sixties, and even with the advent of major hydroelectric developments in the southern watersheds (Prinsenberg, 1980) research interest focussed mainly on the inshore areas directly affected by the projects. Summer data were collected to document the pre-development baseline condition within James Bay, and to a lesser extent within Hudson Bay. Winter data were collected only from inshore areas of the southeastern part of Hudson Bay while no oceanographic data were collected from the region for the spring and fall periods when the seasonal ice cover forms and breaks up. The large freshwater input by ice melt and run-off occurs in the spring when minimum wind stress conditions prevail, while maximum cooling and large wind stress conditions occur together in the fall, followed by a large salt rejection during the early part of the ice growth period. No data are available for these periods. The sparse data warrant only the usage of simple models to study the sensitivity of the system to man-made changes in the natural cycle of boundary forces such as the run-off.

2 Theory

One-dimensional mixed-layer models are used for areas where the vertical exchange processes between the air and the sea, and the vertical mixing within the water column, affect the local conditions much more rapidly than horizontal advection and mixing. Existing models were reviewed in a paper by Niiler and Kraus (1977), in which most of the equations used in this paper were derived in more detail. The energy equation (1) describing the deepening of the surface mixed layer as shown by Niiler and Kraus (1977) is an expansion of the original Kraus and Turner model.

$$\tfrac{1}{2}\frac{dh}{dt}\left(\Delta bh - s|V_s - V_b|^2\right) = mU_*^3 + \tfrac{1}{2}B_0h - \epsilon_0 h \qquad (1)$$

$$\qquad\quad B \qquad\quad C \qquad\quad\quad D \qquad E \qquad H$$

The surface mixed layer has a depth h, a density ρ and moves with a velocity V_s over a deeper layer whose velocity is V_b and density ρ_r. The term b is the buoyancy, U_* the frictional velocity, B_0 the surface buoyancy flux and s, m and ϵ_0 are constants derived from observations. The buoyancy b is related to the density of the surface layer (subscript 0) and of the deep reference layer (subscript r) by:

$$b = g\left(\frac{\rho_r - \rho_0}{\rho_r}\right) = g[\alpha(T_0 - T_r) + \beta(S_r - S_0)] \qquad (2)$$

where a linear approximation of the relation of density to temperature T and salinity S was used and g is the acceleration constant of gravity. The expansion coefficients α and β are functions of salinity and temperature; they vary greatly when maximum density is approached. The surface buoyancy flux B_0 of (1) is a measure of the potential energy supplied to the surface layer through the air-sea interface and is related to the mass flux F_m and the heat flux F_h by:

$$B_0 = \frac{g}{\rho_0} \left(\frac{\alpha}{C} F_h + \beta S_0 F_m \right) \tag{3}$$

where S_0 is the surface salinity value and C is the specific heat constant. A positive heat flux indicates that the surface water is cooled and becomes heavier, resulting in a positive buoyancy flux. When the mass flux is positive, salt is left behind as the water evaporates, making the remaining water even heavier. In both cases, the potential energy of the surface layer increases, which is used to deepen the surface layer. The heat and mass fluxes also change the surface layer salinity (S_0) and temperature (T_0) values by:

$$\frac{dT_0}{dt} = -\frac{dh}{dt}\frac{\Delta T}{h} - \frac{1}{\rho C h} F_h \tag{4}$$

$$\frac{dS_0}{dt} = -\frac{dh}{dt}\frac{\Delta S}{h} + \frac{S_0}{\rho h} F_m \tag{5}$$

where ΔS and ΔT are the respective changes in salinity and temperature at the mixed-layer depth h with ΔS being negative and ΔT positive for an upwards z-axis.

The frictional velocity U_* is found from the velocity of the air U_a by:

$$\frac{\tau_0}{\rho_0} = U_*^2 = \frac{\rho_a}{\rho_0}(1.00 + 0.07|U_a|) U_a^2 \times 10^{-3} \tag{6}$$

where ρ_a and ρ_0 are the densities of air and water, respectively, and where U_a is in units of metres per second. For a $10\,\mathrm{m\,s^{-1}}$ wind speed (20 knots) and a $10°C$ air temperature, the frictional velocity has a value of $1.4\,\mathrm{cm\,s^{-1}}$.

The parameters of the energy equation (1) can now be defined:

B – Work per unit time needed to lift the dense entrained water and mix it through the upper layer. The buoyancy change Δb refers to the change occurring at the same depth h as for ΔT and ΔS in Eqs (4) and (5).

C – Rate at which energy of the mean velocity field is reduced by mixing across the interface between the surface and bottom layers.

D – Rate of work done by the wind during open water conditions or by tidal friction during ice-covered conditions.

E – Rate of potential energy change produced by the mass and heat fluxes across the air-sea interface.

H – Dissipation of energy of the surface layer. It is assumed to be linearly proportional to the thickness of the surface layer depth h.

Equation (1) can be simplified for Hudson Bay when a time-scale of half a day or
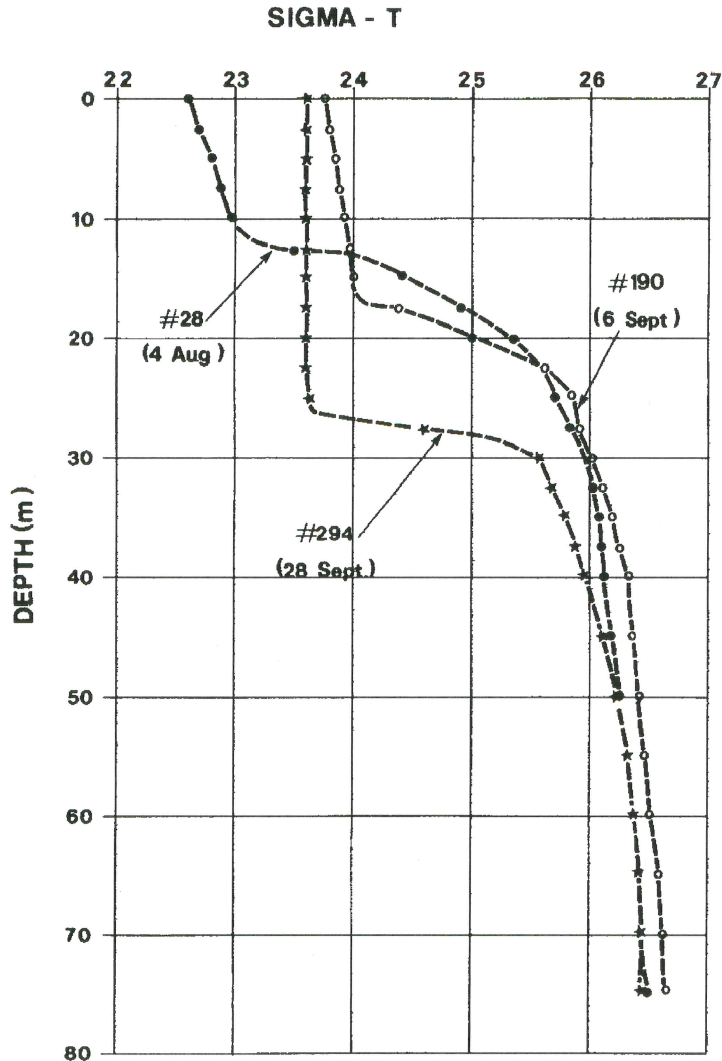
SIGMA - T

Fig 1   Observed summer density profiles for the centre of Hudson Bay (1975)

longer is used The term C, which is caused by the velocity shear, has a maximum effect at half a pendulum day, which equals 7 0 h for latitudes in Hudson Bay The depth (inertial pycnocline depth) attained by this balance of turbulence and buoyancy flux is given by

$$h_1 = \frac{U_*}{N} \, (2N/f)^{1/2} s^{1/4} \tag{7}$$

where the buoyancy term is related to the Brunt-Vaisala frequency $N = (\partial b / \partial z)^{1/2}$ For summer storm conditions in Hudson Bay ($N = 1\,0 \times 10^{-2}\,\mathrm{s}^{-1}$ and $U_* = 2\,0\,\mathrm{cm\,s}^{-1}$), the pycnocline depth would be $17\frac{1}{4}$ m when a constant value of 0 7 is used for s These depths are observed in Hudson Bay (Prinsenberg, 1977a) and increase to 30 m in the fall as shown in Fig 1 The inertial depth h_1 will be used as a minimum value for the pycnocline depth in the model, which uses half-day time steps The term C in (1) is thus omitted, but its effect is included by means of a minimum boundary condition for h at each time step
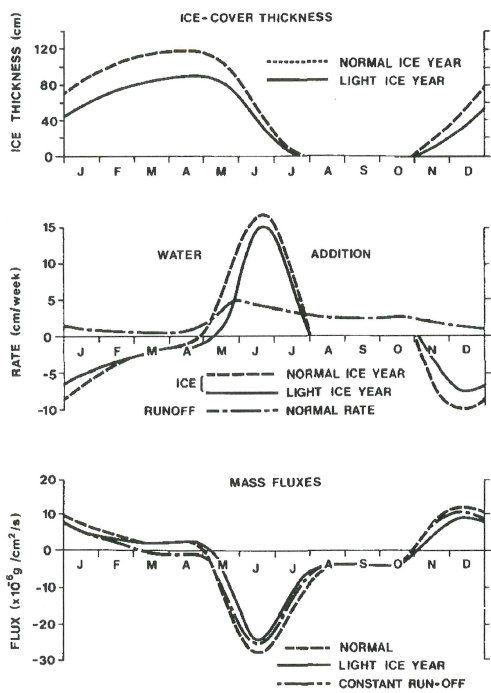
Fig 2 Seasonal pattern of the ice thickness, water addition and mass flux for Hudson Bay
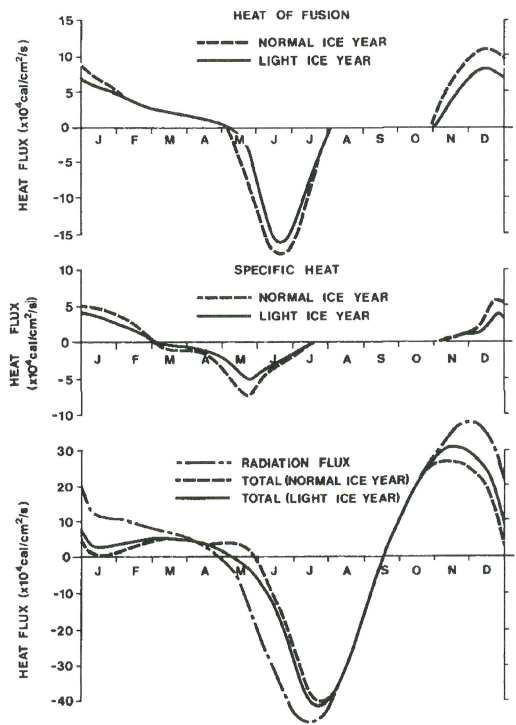

Fig 3 Seasonal pattern of heat fusion and specific heat of the ice cover, and the total heat flux to and from the surface water of Hudson Bay

3 Surface fluxes

Buoyancy flux is a measure of the rate of change of the surface layer density. The density depends upon salinity and temperature through the linear constants α and β (Eq. (2)). The salinity constant β remains invariant at 0.7908 in sigma-t units per ‰ over the temperature and salinity ranges encountered in Hudson Bay. On the other hand, the value of α, the temperature constant, varies greatly with temperature. For Hudson Bay the values of α (in units of $°C^{-1}$) can be obtained from Knudsen's table (e.g. Oxner and Knudsen, 1962) or by the following derived equation:

$$\alpha = \left[3.2(S - 30) + 15(T + 3) - \left(0.17 + \frac{S - 30}{120} \right)(T + 3)^2 \right] \times 10^{-6} \quad (8)$$

It changes by a factor of 10 from $0.018 \times 10^{-3}\,°C^{-1}$ to $0.1326 \times 10^{-3}\,°C^{-1}$ as the mean temperature increases from $-0.5°C$ to $7.5°C$. So although density is written as a simple linear expansion of S and T, the model actually uses higher powers of S and T via α and β in the computation of the density and the mass flux.

Danielson (1969) obtained values of the heat flux (F_h) for Hudson Bay. These and the freshwater input rates (Prinsenberg, 1977b) will be used as the air-sea interface boundary conditions from which the buoyancy flux is calculated by means of Eq. (3). F_h and F_m are only available as mean monthly values, from which daily values were interpolated (Figs 2 and 3). Open water conditions exist during August and September, with partly open water conditions in July, November and December. During open water conditions the mass flux comprises only the run-off contribution which includes evaporation and precipitation. It is negative, indicating a net addition of water, which dilutes the surface layer. The heat flux changes rapidly during this period from a peak negative value (heating) to a large positive value (cooling). It first opposes the deepening of the pycnocline, and later reinforces it; the mass flux opposes the deepening throughout the open water period. The figures also show curves for two other cases: (1) a light ice year when the ice-cover thickness is reduced by 25%, and (2) a constant run-off year. These cases are used to study the sensitivity of the system to changes caused by hydroelectric developments and to changes in the annual ice cover.

In a complete model, the heat flux through the air-sea boundary would determine the start and rate of freezing after the water of the surface layer has been cooled to its freezing point. This is beyond the scope of the present simple mixed-layer model. For now, the ice thickness is assumed to be a function of time so that the heat and mass needed to obtain it can be calculated. Ice accretion starts in November and reaches a maximum thickness of 1.2 m at the end of April. If a 5‰ salinity content is assumed for the ice, then this would mean that a freshwater layer of 0.92 m makes up the ice cover. Results from the ice model by Maykut (1978) have shown that in the early winter a large amount of heat leaves the water and ice medium and causes the ice cover to build up rapidly, insulating the water from the air. Figure 2 shows the thickness of the seasonal ice cover used in the heat and mass flux calculations. The buoyancy flux during the ice accretion period is mainly caused by the mass flux, since the heat flux contribution becomes small after the ice cover is established. Melting of the ice cover will begin at the end of April and continue until the end of July. During

the early spring the run-off contribution also increases and the two processes reinforce each other, decreasing the density of the surface layer. Both the mass and heat fluxes are negative (into the water), producing a negative buoyancy flux, and making the surface layer water lighter.

Figure 2 shows the effects of the hydroelectric developments on the total mass flux assuming a constant year-round run-off. Although less water is removed from the surface layer during the ice accretion period owing to the increased run-off, the mass flux is still positive. The change-over period from a positive to a negative mass flux will be earlier in the spring than before, and the spring peak value of the mass flux will be reduced since the run-off will be less during the spring freshet. The case of reduced ice-cover thickness shows similar deviations from the normal ice-cover year. The mass flux is reduced in the fall and spring while less water is removed and returned to the annual ice cover. Figure 3 shows the heat fluxes as a function of time for the two ice-cover cases. The heat of fusion represents the heat transferred to and from the ice cover to build or melt it while the specific heat represents the heat required to bring it to its melting temperature. Both fluxes change as the ice-cover thickness is altered, thus modifying the total seasonal heat flux cycle shown at the bottom of Figure 3. As less ice is formed, more heat is removed from the surface layer; conversely, as less ice has to be melted, more heat is added.

During open water conditions the frictional velocity U_* is related to the wind stress by (6). In practice, wind data are observed at hourly or at three- or six-hour intervals, from which monthly histograms and mean values are derived (Canadian Government, 1968). Depending on the time step used, the value of the wind speed for (6) has to be a representative value over that time step rather than a vector average. It is calculated by:

$$\rho U_*^2 = (\tau_x^2 + (\tau_x')^2 + \tau_y^2 + (\tau_y')^2)^{1/2} \tag{9}$$

where τ is the mean and τ' is the standard deviation of the stress component. For Hudson Bay only land-based wind data are available; if these are used for offshore areas they must be modified to take into account the general increase of wind speed over open water relative to that over land. The wind speed will be increased by 15%.

During ice-covered conditions it is assumed the ice does not move or moves much more slowly than the tidal currents, so that the currents will generate a stress on the ice cover. The AIDJEX results (McPhee, 1979) have shown that a relationship exists between the current under the ice V and the ice-sea stress τ:

$$\tau = 0.010 V^{1.78} \tag{10}$$

where V is in centimetres per second. This relationship is used to calculate τ and from it U_* by (6). For typical tidal currents (Prinsenberg and Deys, 1979) made up of diurnal and semidiurnal tides having a mean tidal current amplitude of $20 \, \mathrm{cm \, s^{-1}}$, it would give a surface stress of $2.06 \, \mathrm{dynes \, cm^{-2}}$ and a corresponding frictional velocity of $1.42 \, \mathrm{cm \, s^{-1}}$. A storm would produce a stress of similar magnitude. Thus tidal friction underneath an ice cover causes deepening of the surface layer to the same extent that storms do during the fall months.

4 Model results

To obtain smoother profiles and allow fresh water and heat to diffuse into deeper layers, background vertical diffusion of heat and salt were created by:

$$\frac{dT}{dt} = K \frac{d^2T}{dz^2} \tag{11}$$

$$\frac{dS}{dt} = K \frac{d^2S}{dz^2} \tag{12}$$

This refinement to the mixed-layer model improved the profile results but did not alter the sensitivity of the system to outside forcing. The diffusion at the surface and bottom is forced to zero so that salt and heat are conserved in the total column. To ensure that the model will return to the same starting freshwater and heat content, the surface input of heat and mass over one entire year must be zero. No adjustments can be made through side boundaries by horizontal transports. When the heat flux was originally integrated there was a small net yearly heat flux into the bay of $0.425 \times 10^{-4}\,\mathrm{cal\,s^{-1}\,cm^{-2}}$. Since heat is mainly transported out of the bay by the summer surface outflow, the values of the heat flux over the three summer months were decreased by $1.7 \times 10^{-4}\,\mathrm{cal\,s^{-1}\,cm^{-2}}$ so that there would be a net zero annual heat input. This is a small adjustment compared to the total heat flux value but it allowed the model to return to the same heat content value after a yearly cycle.

A similar simple adjustment cannot be applied to the mass flux, whose yearly average value is $-2.98 \times 10^{-6}\,\mathrm{g\,s^{-1}\,cm^{-2}}$. If one reduced the mass flux values of the summer and winter according to the outflow of the bay, one would in effect take away the run-off contribution leaving only the ice accretion and ablation contribution. This would not truly represent the physics of the pycnocline energy balance. To keep the proper cyclic magnitude of the mass flux as a driving force in the pycnocline development, but at the same time come back to the same freshwater content after a one-year cycle, the model readjusts the salinity values after each time step. They are adjusted by a constant value so that the mean salinity value follows a predetermined yearly pattern. The model thus will influence the relative structure of the profiles but not the absolute value of the salinity. The yearly mean salinity pattern for Hudson Bay is given by:

$$\bar{S} = 32.39 + 0.2 \sin\left[\frac{2\pi}{365}(t - 30)\right] \tag{13}$$

where t is the time in Julian days; (13) was derived from the observed seasonal pattern at the entrance of James Bay (Prinsenberg, 1978).

For Hudson Bay, the model used half-day time and 1-m depth intervals. The yearly cycle was started at Julian Day 216 (August 4) for which salinity and temperature data are available (Fig. 1). The model parameters (ϵ_0 and K) were adjusted until the results closely matched those observed at Julian Day 271, attained a maximum pycnocline depth in the range of 60 to 80 m, and returned as closely as possible to the starting properties after a one-year cycle. This maximum pycnocline depth range was
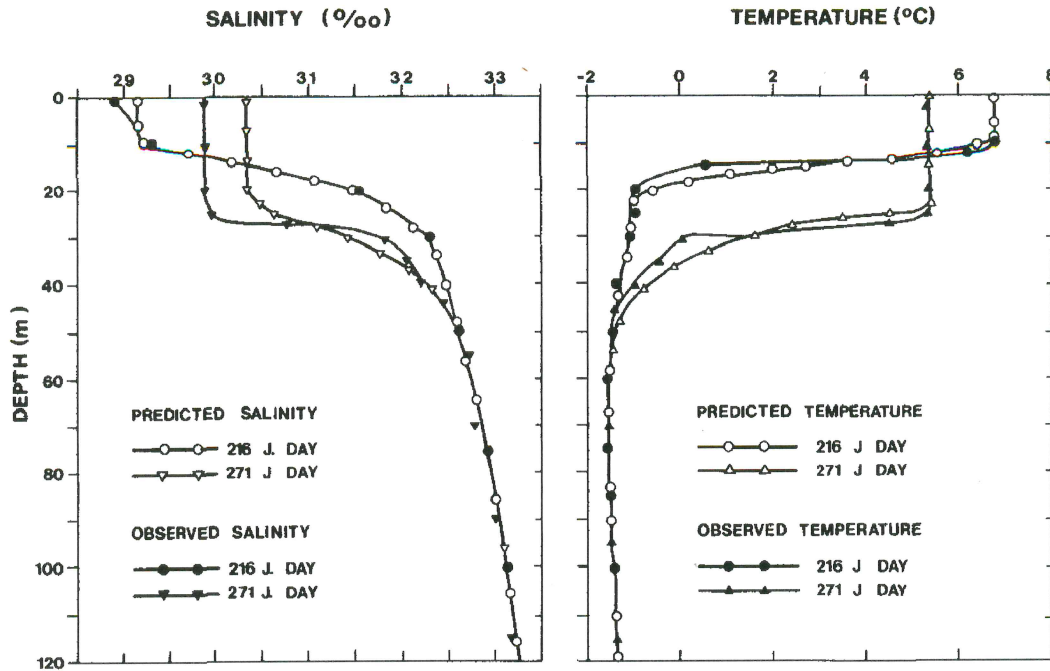
SALINITY (‰)   TEMPERATURE (°C)

Fig. 4   Observed and predicted salinity and temperature profiles for the centre of Hudson Bay.

determined from winter data of the southeastern part of the bay and from pycnocline remnants observed at large depths in the summer data. The final parameters were $0.08\,\mathrm{cm^2\,s^{-1}}$ for the diffusion coefficient K and $0.0035\,\mathrm{cm^2\,s^{-3}}$ for the background friction constant ϵ_0 and were also used for the light ice year and constant run-off cases.

Figure 4 shows the observed and predicted temperature and salinity profiles for Hudson Bay on Julian Day 216 and Julian Day 271. During this period (August 4 to September 29), the mass flux is very constant while the heat flux is decreasing rapidly from its summer maximum. Although the heat content of the surface layer has nearly doubled over the period, the surface layer temperature actually decreases from 6.75°C to 5.35°C, as the pycnocline depth more than doubles. The predicted temperatures profile does agree well with the observed profile; however, the salinity profile does not. The predicted salinity surface value at Julian Day 271 is 0.45‰ higher than the observed value, thus requiring a larger freshwater input than used. This indicates the problem of treating run-off as an air-sea interface phenomenon with a freshwater sink distributed over the total water column.

The summer results of the one-dimensional model, however, were encouraging enough to study the contributions of the fluxes to the yearly pycnocline cycle. Figure 5 shows just the salinity profiles at 30-day intervals and reveals a gradual deepening of the pycnocline throughout the summer, fall and early winter. The model started on August 4 after the large freshwater inputs of the ice melt (Julian Day 170) and run-off (Julian Day 145) had passed and just after the peak in the heat flux (Julian Day 195). At this time the surface salinity is at a minimum while the surface temperature is approaching its maximum value. As the summer progresses, the wind stress increases as the heat and run-off inputs decrease, all causing the pycnocline depth to increase. This continues in the fall and early winter, when large wind stresses and a great
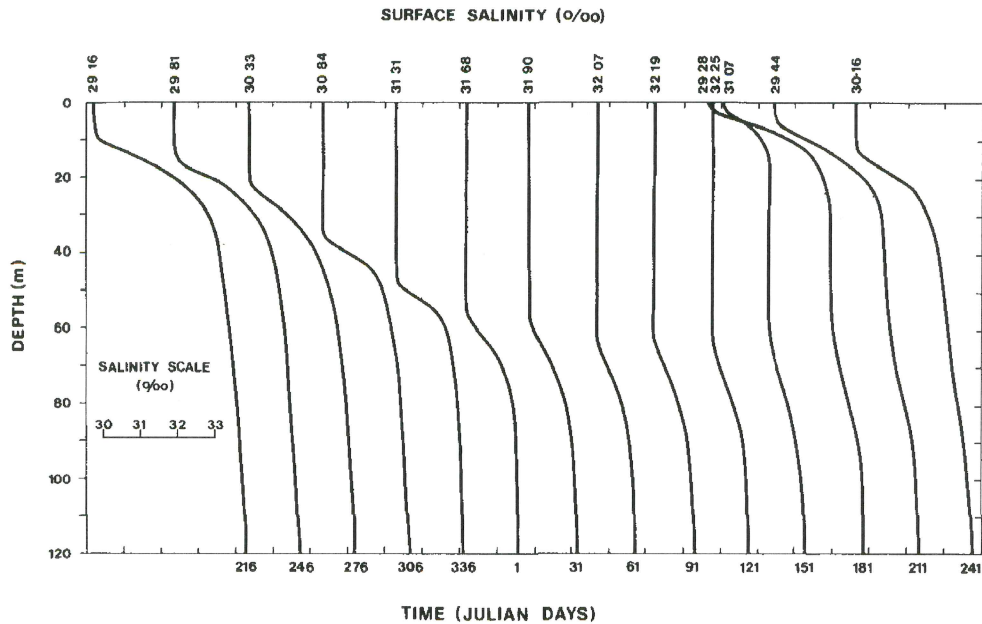
SURFACE SALINITY (o/oo)

Fig. 5   Predicted salinity profiles at a thirty-day time interval for a one-year period.

amount of cooling occurs, followed by salt rejection during the buildup of the seasonal ice cover. During the winter months of February, March and April (Julian Days 31 to 121) the profile structures do not alter too much since both the mass and the heat fluxes are small and very constant. The deepening effect of the reduced salt rejection and tidal mixing is balanced by the background dissipation.

After the first of May (Julian Day 121), the mass flux changes direction as the run-off increases and offsets the freshwater removal by ice accretion. The reduced buoyancy cannot maintain the deep pycnocline and a new shallow halocline is formed whose depth is given by the minimum value calculated from Eq. (7). As the mass flux increases because of ice melt, the surface layer salinity decreases rapidly and the surface temperature starts to increase. During the month of July (Julian Days 181 to 211) the heat flux reaches its maximum value, which melts the ice cover as well as heats the surface layer. A stable surface layer of less saline and warm water is formed, reaching a depth of 10 m before the ice cover disappears and wind mixing deepens the layer to 15 m (Julian Day 241). In the meantime, the old pycnocline at 65 m slowly loses its identity owing to vertical diffusion.

Figure 5 provides a good representation of the changes that occur in the vertical structure with time but not the actual change in magnitude. This is shown to better advantage in Fig. 6, where the surface values of salinity, temperature and pycnocline depth are plotted for a normal year (pre-project), light ice year and constant run-off year (post-project). The observed values for the centre of the bay are only available for the months of August and September and are denoted by range bars (Prinsenberg, 1977a). Although the model does reproduce these data, it has some problem returning to the starting values after a one-year cycle. If more diffusion is used the end temperature could be made equal to the starting temperature, but then the difference in salinity values would be even larger.
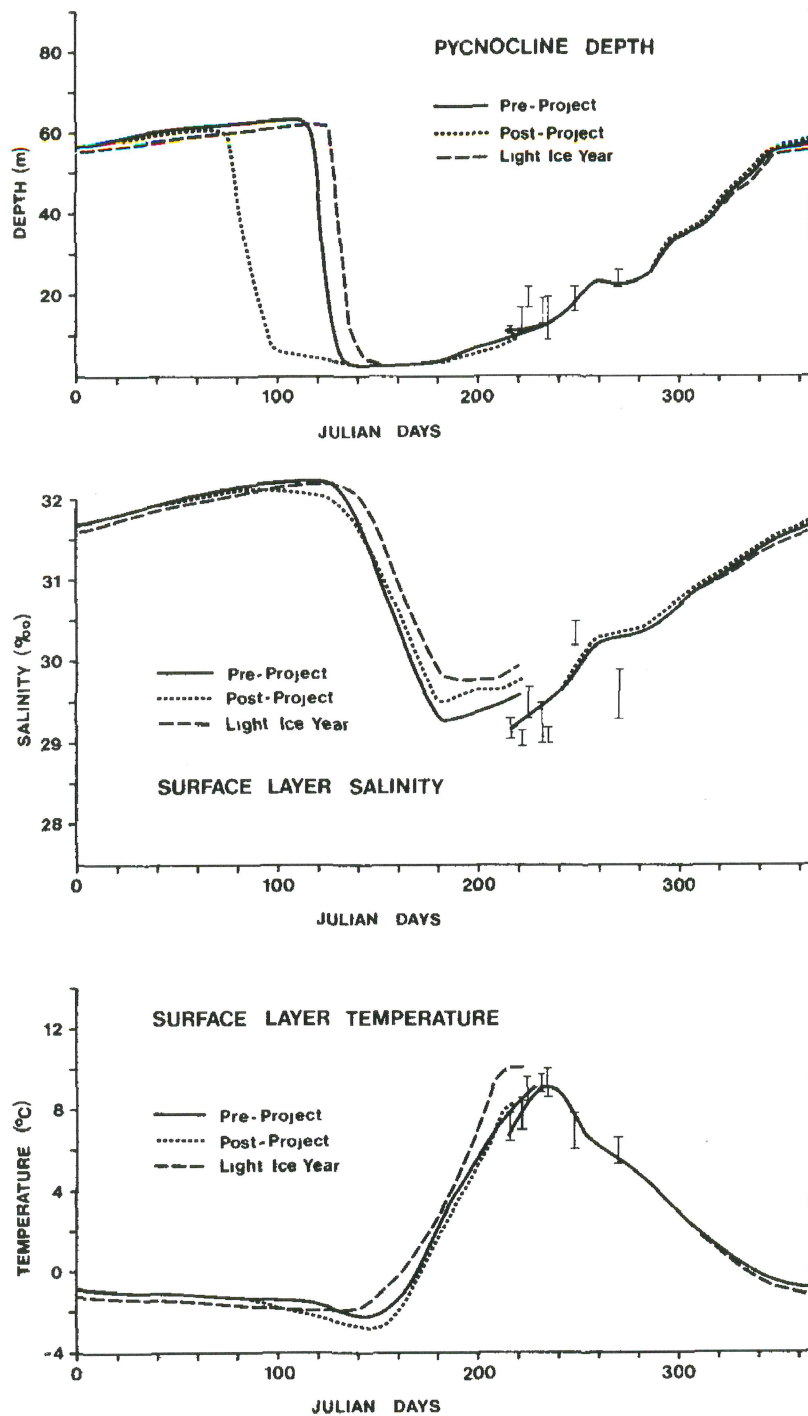
Fig 6 Predicted seasonal pattern of pycnocline depth and surface layer salinity and temperature values for normal year (pre-project), constant run-off (post-project) and light ice year cases.

The model was further used to study the sensitivity of Hudson Bay to variations in the run-off and ice-cover patterns. As the same summer starting conditions were used, no change between the three curves can be seen until the fall. Then, for the light-ice-year case, the reduction of salt rejection from ice accretion causes less deepening of the pycnocline and a smaller increase in surface salinity. The reduction in freezing also causes more cooling of the water, lowering its temperature. The

temperature continues to be lower in the winter, but increases more rapidly in the spring since less ice has to be melted than in a normal year. The depth of the pycnocline increases more slowly throughout the winter since less salt is rejected, and decreases later in the spring to the minimum inertial depth since the shallower maximum attained depth takes less energy to maintain than a deeper one. The surface salinity is thus lower in the winter but higher in the spring since less ice is melted.

The larger run-off of the post-project case reduces the deepening rate of the pycnocline and the rate of increase of the surface salinity during the winter. In the later part of the winter the pycnocline depth and surface salinity are less than those found during a normal year. The new shallow surface pycnocline is established earlier since the mass flux contribution by run-off is larger and overrides the mass flux contribution by freezing earlier. The spring minimum inertial depth of the surface layer appears earlier, but the change-over is slower in response to a slower change in mass flux. As the run-off now enters a stably stratified medium, the surface salinity is lower throughout the winter and also during the spring, even though the spring's run-off magnitude is now reduced.

The variations between the three cases are small compared to the seasonal variation of each case, but indicate the sensitivity of the surface parameters to changes caused by a light ice cover and run-off modification. During the winter the run-off modifications due to the hydroelectric developments cause an earlier return of the shallow surface pycnocline since the run-off contribution to the mass flux offsets the ice accretion contribution earlier. The surface salinity and the temperature both will experience a decrease from their normal winter values. This temperature effect may indicate that there is a tendency to produce more ice than in a normal year since the deep layer heat source will be better isolated from the surface, while surface cooling still persists. In the summer the surface layer salinity will be higher and the temperature lower than for a normal run-off cycle. This will decrease the stability, which will stimulate deepening of the pycnocline and thus cause further deviations from normal conditions.

5 Conclusions

For Hudson Bay, a one-dimensional mixed-layer model was used to study the relative importance of the run-off and ice cover on the seasonal pattern of the pycnocline and the sensitivity of Hudson Bay to their variations. However, to use the model as a predictive tool is unrealistic at this time. First, there is not enough year-round data to calibrate any model and second, many improvements to the model are needed before it can accurately determine magnitudinal changes. Future improvements should address the coupling of the marine environment with the ice cover and with the overlying air mass. The present model specifies the ice-cover growth and decay rather than lets it be determined through the heat budget. Also, in the post-hydroelectric development case, the increased surface stability decreases the heat flux from below and lets the surface layer water fall unrealistically below the freezing point. A coupled model would increase the ice accretion rate instead. Another problem is the coverage of the ice and its movement relative to the water surface. Presently it is taken as fixed in place, although the stress contribution by wind and ice is calculated according to the fractional ice cover. The model thus uses the ice-cover information in the stress

calculation but does not account for the movement of the ice, and thus will overestimate the stress in the fall and spring. The problem of treating the run-off as a surface flux was mentioned in the text itself; it is difficult to get around this without going to multi-dimensional models. Thus, many improvements should be made to the model before one could predict the magnitudinal changes that would occur in the ocean climate as well as in the air climate of the Hudson Bay region that are caused by man-made changes in the run-off cycle.

Acknowledgements

References

BARBER, F G 1967 A contribution to the oceanography of Hudson Bay Manuscr Rep Ser No 4, Marine Sciences Branch, Dep of Mines and Technical Surveys, Ottawa, Ont , 68 pp

CANADIAN GOVERNMENT 1968 Climatic Normals Vol 5, Wind Meteorological Branch, Dep of Transport, Toronto, Ont , 95 pp

DANIELSON, E W , JR 1969 The surface heat budget of Hudson Bay Manuscr Rep No 9, McGill University, Montréal, P Q , 196 pp

MAYKUT, G A 1978 Energy exchange over young sea ice in the central Arctic *J Geophys Res* **83** 3646–3658

McPHEE, M G 1979 The effect of the oceanic boundary layer on the mean drift of pack ice Application of a simple model *J Phys Oceanogr* **9** 388–400

NIILER, P P and E B KRAUS 1977 One-dimensional models of the upper ocean In *Modelling and Prediction of the Upper Layers of the Ocean*, E B Kraus (Ed), Pergamon Press, pp 143–172

OXNER, M and M KNUDSEN 1962 *The Determination of Chlorinity by the Knudsen Method* G M Manufacturing Co , New York N Y , 63 pp

PRINSENBERG, S J 1977a Hudson Bay oceanographic data report 1975. Vol I Data Rep. Ser. No 77-1, Ocean and Aquatic Sciences, Environment Canada, Burlington, Ont , 308 pp

————— 1977b Freshwater budget of Hudson Bay Manuscr Rep Ser No 5, Ocean and Aquatic Sciences Fisheries and Environment Canada, Burlington, Ont , 71 pp

————— 1978 Analytical study of the circulation of James Bay Manuscr Rep Ser No 6, Ocean and Aquatic Sciences, Fisheries and Environment Canada, Burlington, Ont , 55 pp

————— and F W DEYS 1979 Hudson Bay Oceanographic Data Report 1975 Vol 2 Data Rep Ser No 79-4 Ocean and Aquatic Sciences, Fisheries and Oceans, Burlington, Ont , 191 pp

————— 1980 Man-made changes in the freshwater input rates of Hudson and James Bay *Can J. Fish. Aquat. Sci.* **37** 1101–1110